FITEE

Electrically tunable liquid crystal coplanar waveguide stepped-impedance resonator[*]

Xingye FAN[§1], Ruozhou LI[§1,2], Jing YAN[†‡1], Yuming FANG[1,2], Ying YU[†‡1,2]

[1]College of Electronic and Optical Engineering & College of Microelectronics,

Nanjing University of Posts and Telecommunications, Nanjing 210023, China

[2]National and Local Joint Engineering Laboratory of RF Integration and Micro-Assembly Technology,

Nanjing University of Posts and Telecommunications, Nanjing 210023, China

[†]E-mail: jing.yan@njupt.edu.cn; ying_yu_001@163.com

Received June 9, 2020; Revision accepted Nov. 17, 2020; Crosschecked Aug. 24, 2021

Abstract: A tunable stepped-impedance resonator using liquid crystal is demonstrated. Two resonant frequencies at 3.367 and 7.198 GHz are realized and can be continuously tuned by external applied voltages. Continuous tunable ranges of 52 and 210 MHz have been achieved at a particularly low driving voltage of 14 V, which shows good agreement with the simulation results. The voltage-induced hysteresis phenomenon is also investigated. This device also has a low insertion loss of −2.9 and −4 dB for the two resonant frequencies and the return losses are less than −21.5 dB. This work provides a new protocol to realize a tunable frequency for communication systems.

1 Introduction

With the fast development of mobile phones, Bluetooth, Wi-Fi, and other communication devices, the requirements for broadband, multi-frequency, frequency modulational radio frequency (RF) devices are significantly increased. In particular, resonators are considered as the key elements within the devices. Conventional methods use varactor diodes, PIN diodes, ferroelectric materials, and micro-electro-mechanical system (MEMS) elements to tune the resonators (Navarro and Chang, 1993; Semenov et al., 2006; Ustinov et al., 2006; Liu XG et al., 2009; Stefanini et al., 2011; Shi et al., 2017; Teng et al., 2019; Bi et al., 2020). Recently, liquid crystal has emerged as a promising technological advancement for tunable and reconfigurable microwave devices due to its attractive features such as significant electrical tunable permittivity, light weight, low cost, no moving part, and low power consumption.

Several liquid-crystal-based resonators designed for frequency tuning have been proposed (Maune et al., 2003; Mirfatah and Laurin, 2009; Cai et al., 2010; Yaghmaee et al., 2012a, 2012b; Huang et al., 2014; Liu YP et al., 2016; Jiang et al., 2019). At the optical frequency, Maune et al. (2003) demonstrated an electrically tunable ring resonator using nematic liquid crystal as the cladding. The resonator could be

reversibly controlled up to a 0.22-nm tuning range by applying an electric field across the resonator to align the cladding. Cai et al. (2010) experimentally realized an electrically tunable microring resonator (MRR) using a liquid-crystal-clad polymer waveguide. A large tuning range of 0.73 nm was obtained for TE mode at a low operating voltage of 10 V with the threshold voltage of only 3 V. At the microwave frequency, Yaghmaee et al. (2012a) designed an S-band multi-layered tunable stepped-impedance resonator (SIR) with a frequency shift of 140 MHz from 3.3 to 3.16 GHz. Liu YP et al. (2016) proposed a microwave continuously tunable split ring resonator (SRR) band-pass filter using nematic liquid crystal with a bias voltage of 20 V. A complementary SRR band-pass filter with a tuning range of 0.65 GHz from 16.41 to 17.06 GHz was also reported by Jiang et al. (2019), and the bias voltage is 22 V.

A coplanar waveguide (CPW) is a planar transmission line. The central conductor and ground planes of the CPW are located on the same plane, which is conducive to the series or parallel connection of components on the same side. Thus, a simple structure of tunable CPW SIR would further promote the functionalities of wireless communication devices.

In this paper, an electrically tunable liquid crystal CPW SIR is proposed and experimentally realized. Two resonant frequencies at 3.367 and 7.198 GHz are obtained, and can be tuned at a maximum frequency range of 57 and 223 MHz when the bias voltage varies from 0 to 28 V. The experimental results are consistent with the simulation ones. In addition to electrical tunability, this tunable resonator demonstrates benefits such as convenient fabrication, low cost, low power consumption, and low insertion loss. The phenomenon of voltage-induced hysteresis is also investigated. This work provides a new way to generate a tunable frequency for communication systems.

2 Structure design and theoretical analysis

The structure of the proposed liquid-crystal-based CPW SIR is depicted in Fig. 1a. The liquid crystal layer is sandwiched between two substrates. The bottom substrate is a 0.5-mm-thick Rogers RO4003 dielectric substrate covered with a square

copper patch. The length and width of the bottom substrate are 40 and 25 mm, respectively. The top substrate consists of a patterned copper patch on a Rogers RO4003 dielectric substrate of 0.5-mm thickness, and the copper patch is a CPW transmission line as Fig. 1b shows. The bottom and top substrates are cross-assembled. Thus, a two-section SIR is formed. In our designed structure, the patterned copper patch is a CPW transmission line with a high impedance of 50 Ω at both ends, which is substantially matched to the ideal feedline impedance. The middle part of the structure is combined with the liquid crystal layer, and the bottom substrate is a low-impedance coplanar waveguide with ground (CPWG) transmission line. Assuming that the (relative) dielectric constant of liquid crystal is 2.9, the low impedance of the middle part is about 6.010 Ω when the thickness of the liquid crystal is 0.1 mm. Thus, two different impedance values contribute to form the SIR.
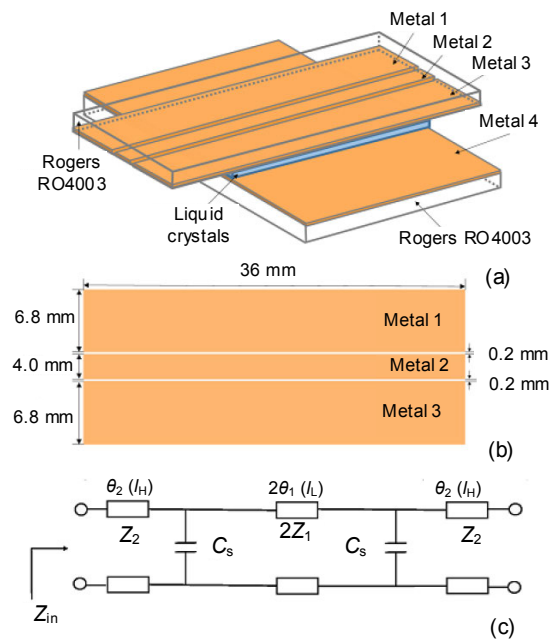
Fig. 1   Schematic of the proposed liquid-crystal-based CPW SIR (a), structure of the transmission line (b), and configuration of the SIR (c)

Fig. 1c shows the equivalent circuit of the proposed three-section stepped-impedance resonator, which consists of two characteristic impedances, electrical lengths of (Z_1; θ_1) and (Z_2; θ_2), and two shunt capacitances C_s at the discontinuity of the SIR. Usually, the shunt capacitances C_s can be ignored to

simplify the model (Simons and Ponchak, 1988). The lengths of the low-impedance line (l_L) and high-impedance line (l_H) are obtained as Z_1=6.010 Ω and Z_2=50 Ω from scattering parameters calculated by simulations for the structure shown in Fig. lb (Sanada et al., 2002). According to transmission line theory, the input impedance of stepped impedance Z_{in} can be expressed as (Makimoto and Yamashita, 1980)

$$Z_{in} = jZ_2 \frac{2(1+K)\tan\theta_1\tan\theta_2 - K(1-\tan^2\theta_2)(1-\tan^2\theta_1)}{2(K-\tan\theta_1\tan\theta_2)(\tan\theta_2 + K\tan\theta_1)},$$
(1)

where

$$K = Z_2 / Z_1,$$
(2)

and the input admittance Y_{in} is

$$Y_{in} = jY_2 \frac{2(K-\tan\theta_1\tan\theta_2)(\tan\theta_2 + K\tan\theta_1)}{2(1+K)\tan\theta_1\tan\theta_2 - K(1-\tan^2\theta_2)(1-\tan^2\theta_1)},$$
(3)

where Y_2 is the admittance of Z_2.

The resonance condition can be obtained from

$$Y_{in} = 0.$$
(4)

From Eqs. (3) and (4), the fundamental resonance condition can be expressed as

$$K - \tan\theta_1\tan\theta_2 = 0.$$
(5)

When the assumed dielectric constant of liquid crystal is 2.9, θ_1, θ_2, and K of this proposed SIR are 86.129°, 29.535°, and 8.374, respectively.

Liquid crystal is a representative stimuli-responsive material with excellent behavior. It is an anisotropic dielectric material and can be continuously tuned by external fields. For the liquid crystal with positive dielectric anisotropy, the liquid crystal molecule trends to align with the electric field, and the dielectric constant can be tuned accordingly because of its anisotropic behavior (Yaghmaee et al., 2013). At the voltage off state (V=0), the equivalent dielectric constant $\bar{\varepsilon}$ of liquid crystal is $(\varepsilon_{//}+2\varepsilon_{\perp})/3$ because the liquid crystal molecules are randomly distributed between the two substrates as shown in Fig. 2a. When an external electric field is added between metal 2 and metal 4 as Fig. 2b illustrates, the liquid crystal molecules trend to be arranged in the direction of the applied field (Yang and Wu, 2006). Thus, the equiv-

alent dielectric constant $\bar{\varepsilon}$ of liquid crystal can be tuned, resulting in the modulation of the resonant frequency of the proposed SIR.
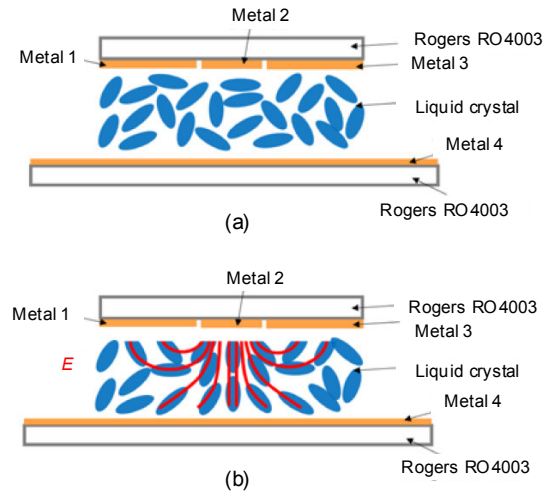
Fig. 2 Liquid crystal molecule distribution of the SIR: (a) voltage off state (V=0); (b) voltage on state (V>0)

To demonstrate that the liquid-crystal-based CPW SIR structure can realize continuous tunability, the software ANSYS HFSS, which is a three-dimensional (3D) electromagnetic simulation software for designing and simulating high-frequency electronic products, is used to simulate the electromagnetic performance of the proposed device at a frequency range from 2.4 to 7.7 GHz, where the liquid crystal materials are regarded as a material with a different defined dielectric constant. The geometric and material parameters used for the simulations are as shown in Fig. 1. The dielectric constant of the liquid crystal is assumed to vary from 2.8 to 3.0. The simulation results of S_{11} and S_{21} spectra at various liquid crystal dielectric constants are shown in Fig. 3. Obviously, it is found that two resonant frequencies are formed in this proposed SIR structure within the frequency range from 2.4 to 7.7 GHz, and the dielectric constant of liquid crystal has significant impact on the resonant frequency. With the increase of the dielectric constant of liquid crystal, both the low and high resonant frequencies shift to a lower band. The low resonant frequency (f_1) can shift by 70 MHz from 3.620 to 3.550 GHz, while a shift of 240 MHz can be obtained from 7.240 to 7.000 GHz for the high resonant frequency (f_2). The simulation results verify that the proposed CPW SIR using liquid crystal can be electrically tuned.
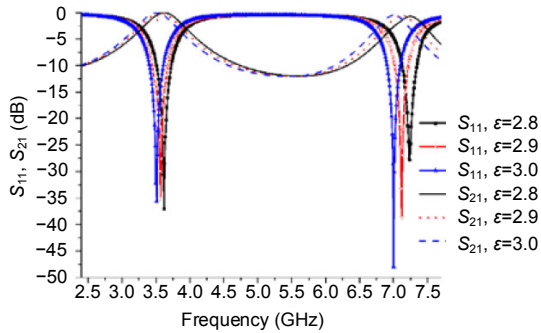
Fig. 3 Simulation results of S_{11} and S_{21} spectra of the SIR when the liquid crystal dielectric constant varies from 2.8 to 3.0

3 Experimental results and discussion

A prototype of the proposed electrically tunable liquid crystal CPW SIR is constructed. According to the simulated results, 0.5-mm Rogers RO4003 substrates (ε_r=3.55, tanδ=0.0027) are used as the top and bottom substrates, where the patterned copper patch is designed on the top substrate. Two stripes of Mylar film are sealed along two parallel edges to separate the substrates, and the thickness of the gap is 0.1 mm. A commercial liquid crystal material, 5CB, is sandwiched between the crossed substrates. For RF performance testing, SubMiniature version A (SMA, pin diameter 1.24 mm, medium diameter 4.10 mm) connectors are used to mount the sample to a cable. Bias tees are incorporated into the test circuit to apply electric fields on the liquid crystal layer. The RF performance of the sample is examined using a vector network analyzer (E5071C, Keysight Technologies, United States) from 9 kHz to 20 GHz. The port impedance of the vector network analyzer is maintained at the standard impendence of 50 Ω. A direct current (DC) voltage source is used to apply electric fields on the liquid crystal layer with a voltage range of 0–30 V.

The experimental results plotted in Fig. 4 illustrate the proposed tunable liquid crystal CPW SIR with the applied voltages of 1, 4, and 24 V. The measurement results agree well with the simulation results as shown in Fig. 4. As expected, two resonant frequencies are formed, and both frequencies can be tuned by external applied voltages. The low resonant frequency f_1 changes from 3.367 to 3.311 GHz when an external voltage of 24 V is applied to the SIR. At the same time, the high resonant frequency f_2 shifts by

221 MHz from 7.198 to 6.977 GHz. The tuning ranges (defined as the relative frequency variation divided by the frequency at 0 V) for f_1 and f_2 are 1.67% and 3.07%, respectively. The S_{11} spectra, which present the reflection of RF signals through the SIR, show that the return loss (S_{11}) for both resonant frequencies is less than −21.5 dB. On the other hand, the S_{21} spectra illustrate the transmission of RF signals and show that the insertion loss (S_{21}) is −2.9 dB for f_1 and −4 dB for f_2; most are introduced by bias tees. By increasing the applied voltage, the S_{11} of the resonant frequencies decreases, while the S_{21} spectra are nearly the same. In addition, the modulation response rate of the system is about several seconds, which is similar to that of a conventional liquid crystal adaptive lens (Algorri et al., 2016).
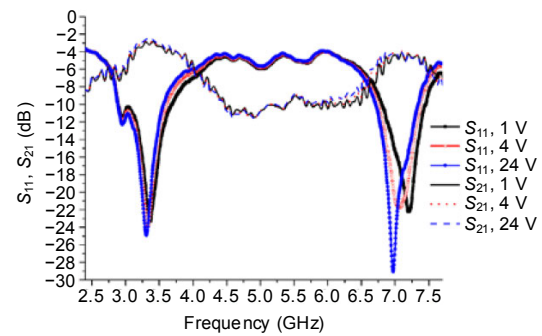
Fig. 4 Experimental results of S_{11} and S_{21} spectra of the SIR when the applied voltage is 1, 4, or 24 V

The experimental results of the resonant frequencies as a function of the applied voltage are plotted in Fig. 5, which clearly shows that the resonant frequency can be continuously tuned. As the applied voltage increases to 28 V, the low resonant frequency f_1 shifts from 3.367 to 3.310 GHz, and the high resonant frequency f_2 can be tuned from 7.198 to 6.975 GHz. As a result, 57 and 223 MHz continuous tunable ranges can be obtained for this SIR. Note that a threshold voltage also exists in this device. Only when the applied voltage exceeds the threshold voltage (V^{th}≈2 V), are liquid crystal molecules reoriented by the applied electric field, which results in a change in the equivalent dielectric constant of the liquid crystal layer (Yang and Wu, 2006). Both the resonant frequencies vary rapidly when the applied voltage exceeds 2 V. The low resonant frequency f_1 rapidly shifts from 3.362 to 3.321 GHz, and the high resonant frequency f_2 can achieve a 186 MHz

continuously tunable range at the same time when the applied voltage varies from 2 to 8 V. After that, both the resonant frequencies change gently with the increase of the applied voltage. Over the entire voltage drive range, both the resonant frequencies can be continuously tuned by the external electric fields. Another noteworthy phenomenon is the presence of the saturation voltage. As the external applied voltage increases to more than 14 V, although the resonant frequency decreases slightly with an increase in voltage, the tuning range is very small. When the applied voltage exceeds 24 V, the resonant frequencies are almost the same, which means that nearly all the liquid crystal molecules are reoriented to be arranged in the direction of the applied electric field. Therefore, in addition to achieving tunability, this architecture can be operated at a particularly low driving voltage (about 14 V) with low power consumption. Continuous tunable ranges of 52 and 210 MHz can been achieved at 14 V.
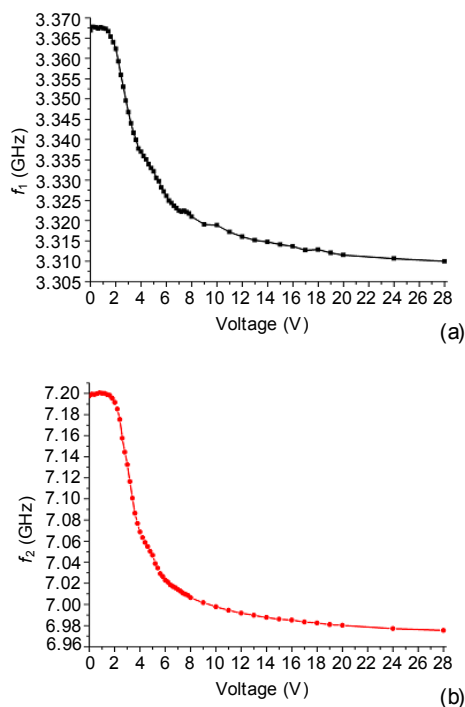
Fig. 5 Experimental results of the resonant frequency as a function of the applied voltage: (a) low resonant frequency f_1; (b) high resonant frequency f_2

Because the liquid crystal CPW SIR structure can realize electrical tunability, we consider the hysteresis phenomenon of the device. We measure the hysteresis loop of the sample under different external

applied voltages by increasing the voltage to a certain level and then decreasing it to zero. The measured hysteresis loops of the resonant frequencies under different electric fields are plotted in Fig. 6, in which solid lines and dashed lines represent the *V-f* (voltage-resonant frequency) curves under forward and backward driving, respectively. Here, we discuss only the hysteresis curves of the high resonant frequency f_2 because of its wide tuning range, while the low resonant frequency f_1 exhibits a similar trend. A quite different hysteresis phenomenon is obtained for this proposed device. For the high resonant frequency f_2, when the external voltage is higher than 4 V, the forward and backward *V-f* curves significantly overlap, so the hysteresis is nearly unnoticeable and the resonant frequencies of the proposed device can be precisely controlled by external voltages. Different from the hysteresis effect in conventional liquid crystal electro-optic devices, which usually have a hysteresis loop at high applied voltage, the hysteresis loop is observed in the low applied voltage range (less than 4 V in this case), as clearly shown in Fig. 6 in this case. This is because no alignment layer is used in this prototype. When external voltage is not applied, the liquid crystal molecules are distributed randomly.
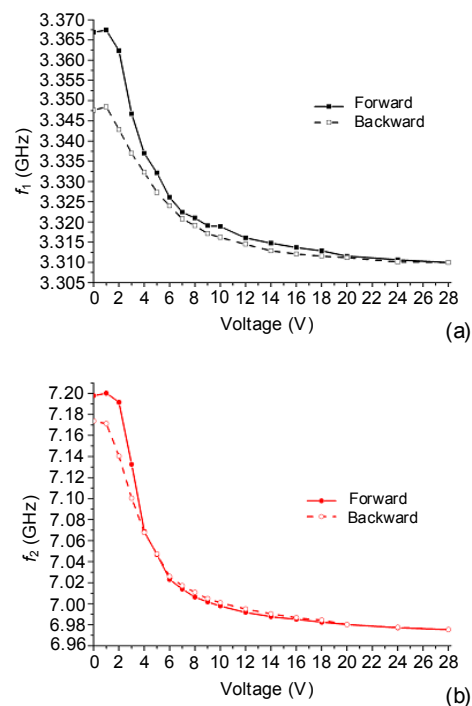
Fig. 6 Measured hysteresis loops of the resonant frequency under different electric fields: (a) low resonant frequency f_1; (b) high resonant frequency f_2

When relatively large voltages (larger than 4 V) are applied to the device, almost all the liquid crystal molecules are arranged in the direction of electric fields in the forward and backward driving schemes. However, because the external voltage is less than 4 V, the electric field cannot maintain the orderly arrangement of all liquid crystal molecules along the electric field direction; some liquid crystal molecules return to a randomly distributed state, leading to the separation of the forward and backward *V-f* curves. One approach for suppressing the hysteresis is to add alignment layers at both surfaces of the substrates; however, the tradeoffs are an increasingly complicated fabrication process and poor alignment performance, because of the large liquid crystal layer thickness.

4 Conclusions

In this paper, we demonstrate an electrically tunable CPW SIR using liquid crystal. Both the resonant frequencies can be continuously tuned by external applied voltages, and the experimental results agree well with the simulation ones. By increasing the applied voltage, the low resonant frequency f_1 can be shifted from 3.367 to 3.310 GHz, while the high resonant frequency f_2 can be tuned from 7.198 to 6.975 GHz. Continuous tunable ranges of 52 and 210 MHz can be achieved for the two resonant frequencies with a relatively low voltage of 14 V. In addition to the properties of convenient fabrication, low cost, and low power consumption, our tunable resonator possesses the characteristic of low insertion loss of −2.9 and −4 dB for the two resonant frequencies, and the return losses are all less than −21.5 dB. The phenomenon of voltage-induced hysteresis is also investigated. The hysteresis loop appears in the low voltage range. This device has great potential in frequency tunable applications of communication systems.

Contributors

Ruozhou LI and Jing YAN designed the research. Xingye FAN and Ruozhou LI conducted the investigation and processed the data. Xingye FAN and Jing YAN drafted the paper. Yuming FANG and Ying YU supervised the research and helped organize the paper. Ruozhou LI and Ying YU revised and finalized the paper.

Compliance with ethics guidelines

Xingye FAN, Ruozhou LI, Jing YAN, Yuming FANG, and Ying YU declare that they have no conflict of interest.

References

Algorri JF, Urruchi V, García-Cámara B, et al., 2016. Liquid crystal microlenses for autostereoscopic displays. *Materials*, 9(1):36. https://doi.org/10.3390/ma9010036

Bi XK, Zhang X, Wong SW, et al., 2020. Design of notched-wideband bandpass filters with reconfigurable bandwidth based on terminated cross-shaped resonators. *IEEE Access*, 8:37416-37427.
https://doi.org/10.1109/ACCESS.2020.2975379

Cai T, Liu QK, Shi YC, et al., 2010. An efficiently tunable microring resonator using a liquid crystal-cladded polymer waveguide. *Appl Phys Lett*, 97(12):121109.
https://doi.org/10.1063/1.3492848

Huang T, Jiang D, Shao ZH, 2014. Research of a novel bandpass filter using nematic liquid crystal loaded by inverted microstrip. IEEE Int Conf on Communication Problem-Solving, p.514-516.
https://doi.org/10.1109/ICCPS.2014.7062336

Jiang D, Liu YP, Li XY, et al., 2019. Tunable microwave bandpass filters with complementary split ring resonator and liquid crystal materials. *IEEE Access*, 7:126265-126272. https://doi.org/10.1109/ACCESS.2019.2924194

Liu XG, Katehi LPB, Chappell WJ, et al., 2009. A 3.4–6.2 GHz continuously tunable electrostatic MEMS resonator with quality factor of 460–530. IEEE MTT-S Int Microwave Symp Digest, p.1149-1152.
https://doi.org/10.1109/MWSYM.2009.5165905

Liu YP, Jiang D, Cao WP, et al., 2016. Microwave tunable split ring resonator bandpass filter using nematic liquid crystal materials. *Optik*, 127(21):10216-10222.
https://doi.org/10.1016/j.ijleo.2016.08.034

Makimoto M, Yamashita S, 1980. Bandpass filters using parallel coupled strip-line stepped impedance resonators. IEEE MTT-S Int Microwave Symp Digest, p.141-143.
https://doi.org/10.1109/MWSYM.1980.1124210

Maune B, Lawson R, Gunn G, et al., 2003. Electrically tunable ring resonators incorporating nematic liquid crystals as cladding layers. *Appl Phys Lett*, 83(23):4689-4691.
https://doi.org/10.1063/1.1630370

Mirfatah A, Laurin JJ, 2009. Tunable hairpin resonator based on liquid crystal. Proc 13th Int Symp on Antenna Technology and Applied Electromagnetics and the Canadian Radio Science Meeting, p.6-9.
https://doi.org/10.1109/ANTEMURSI.2009.4805086

Navarro JA, Chang K, 1993. Varactor-tunable uniplanar ring resonators. *IEEE Trans Microw Theory Techn*, 41(5):760-766. https://doi.org/10.1109/22.234508

Sanada A, Takehara H, Yamamoto T, et al., 2002. λ/4 stepped-impedance resonator bandpass filters fabricated on coplanar waveguide. IEEE MTT-S Int Microwave Symp Digest, p.385-388.
https://doi.org/10.1109/MWSYM.2002.1011636

Semenov AA, Karmanenko SF, Demidov VE, et al., 2006. Ferrite-ferroelectric layered structures for electrically and magnetically tunable microwave resonators. *Appl Phys Lett*, 88(3):033503. https://doi.org/10.1063/1.2166489

Shi ZD, Fang L, Zhong LB, 2017. MEMS-based filter integrating tunable Fabry-Perot cavity and grating. *Opt Commun*, 402:472-477.
https://doi.org/10.1016/j.optcom.2017.06.043

Simons RN, Ponchak GE, 1988. Modeling of some coplanar waveguide discontinuities. IEEE MTT-S Int Microwave Symp Digest, p.297-300.
https://doi.org/10.1109/MWSYM.1988.22035

Stefanini R, Martinez JD, Chatras M, et al., 2011. Ku band high-Q tunable surface-mounted cavity resonator using RF MEMS varactors. *IEEE Microw Wirel Compon Lett*, 21(5):237-239.
https://doi.org/10.1109/LMWC.2011.2126565

Teng C, Cheong P, Tarn KW, 2019. Reconfigurable wideband bandpass filters based on dual cross-shaped resonator. IEEE MTT-S Int Wireless Symp, p.1-3.
https://doi.org/10.1109/IEEE-IWS.2019.8804159

Ustinov AB, Tiberkevich VS, Srinivasan G, et al., 2006. Electric field tunable ferrite-ferroelectric hybrid wave microwave resonators: experiment and theory. *J Appl Phys*, 100(9):093905. https://doi.org/10.1063/1.2372575

Yaghmaee P, Fumeaux C, Bates B, et al., 2012a. Frequency tunable S-band resonator using nematic liquid crystal. *Electron Lett*, 48(13):798-800.
https://doi.org/10.1049/el.2012.1366

Yaghmaee P, Horestani AK, Bates B, et al., 2012b. A multi-layered tunable stepped-impedance resonator for liquid crystal characterization. Asia Pacific Microwave Conf Proc, p.776-778.
https://doi.org/10.1109/APMC.2012.6421732

Yaghmaee P, Karabey OH, Bates B, et al., 2013. Electrically tuned microwave devices using liquid crystal technology. *Int J Antenn Propag*, 2013:824214.
https://doi.org/10.1155/2013/824214

Yang DK, Wu ST, 2006. Effects of electric field on liquid crystals. In: Yang DK, Wu ST (Eds.), Fundamentals of Liquid Crystal Devices. John Wiley, Chichester, p.107-112. https://doi.org/10.1002/0470032030.ch4